

Vibrationally Resolved Decay Width of Interatomic Coulombic Decay in HeNe

F. Trinter,¹ J. B. Williams,¹ M. Weller,¹ M. Waitz,¹ M. Pitzer,¹ J. Voigtsberger,¹ C. Schober,¹ G. Kastirke,¹ C. Müller,¹ C. Goihl,¹ P. Burzynski,¹ F. Wiegandt,¹ R. Wallauer,¹ A. Kalinin,¹ L. Ph. H. Schmidt,¹ M. S. Schöffler,¹ Y.-C. Chiang,² K. Gokhberg,² T. Jahnke,¹ and R. Dörner^{1,*}

¹*Institut für Kernphysik, J. W. Goethe-Universität, Max-von-Laue-Strasse 1, D-60438 Frankfurt am Main, Germany*

²*Theoretische Chemie, Universität Heidelberg, Im Neuenheimer Feld 229, D-69120 Heidelberg, Germany*

(Received 7 July 2013; published 4 December 2013)

We investigate the ionization of HeNe from below the He $1s3p$ excitation to the He ionization threshold. We observe HeNe⁺ ions with an enhancement by more than a factor of 60 when the He side couples resonantly to the radiation field. These ions are an experimental proof of a two-center resonant photoionization mechanism predicted by Najjari *et al.* [Phys. Rev. Lett. **105**, 153002 (2010)]. Furthermore, our data provide electronic and vibrational state resolved decay widths of interatomic Coulombic decay in HeNe dimers. We find that the interatomic Coulombic decay lifetime strongly increases with increasing vibrational state.

DOI: [10.1103/PhysRevLett.111.233004](https://doi.org/10.1103/PhysRevLett.111.233004)

PACS numbers: 33.15.Vb, 36.40.Sx

In radio technology, antennas are used to efficiently collect energy from the electromagnetic field. In the optical regime, nanoscale antennas have been developed [1], and in nature, specialized antenna molecules efficiently collect visible light to power biochemical reactions. Schematically, all these systems consist of the antenna itself, which couples to the radiation field, a receiver which uses the energy, and a route to transport the energy between them.

The linear coupling of light to matter at energies above the ionization threshold shows a smooth energy dependence with stepwise increases whenever a new shell opens. On top of this smooth dependence of the ionization cross section are different types of resonance features. For atoms, most notably, there are, e.g., Fano resonances created by doubly excited states embedded in the continuum [2]. In 2010, Najjari *et al.* [3] predicted that for such a resonant enhancement of the photoionization cross section to occur, the resonant excitation state does not need to be on the same subsystem which finally is ionized. Instead, one atom can act as an antenna which resonantly absorbs the light while a second atom can be the receiver which finally gets ionized. This proposed antenna mechanism for the interaction with the radiation field builds on pioneering work by Gokhberg *et al.* [4], who showed that excitation energy can be transferred from a neutral atom to a neighbor in a process that is similar to interatomic Coulombic decay (ICD) [5–8]. In chemistry, intracluster energy transfer has been studied since the mid-1980s under different names such as intermolecular autoionization [9] or intramolecular Penning ionization [10]. It was also shown that it is feasible to extend this physical scenario of two-center resonant photoionization to molecules [11]. The important question of the time scale of the energy transfer, however, could not be answered until today.

In the present experiment, we demonstrate the smallest possible implementation of an antenna-receiver complex

which consists of a single (helium) atom acting as the antenna and a second (neon) atom acting as a receiver. In this most simple antenna-receiver setup, the antenna atom enhances the coupling to the radiation field by more than a factor of 60. After being collected by the antenna, the energy is transferred to the receiver via ICD. The fact that the studied system consists of just two atoms allows us to investigate the physics of the energy transfer in high detail, i.e., on the level of a single vibrational quantum state, and to measure the energy transfer times. We find that the decay time strongly depends on the vibrational level, which demonstrates the predicted strong dependence on internuclear distance.

For this antenna mechanism to be unambiguously identified in an experiment, the two atoms involved must have significantly different ionization thresholds. The antenna system has to possess an excited bound state with a large oscillator strength which is energetically located above the ionization threshold of the receiver system, as illustrated in Fig. 1. In addition, the energy transfer mechanism has to be fast compared to the radiative relaxation of the antenna. In the present work, we choose the HeNe dimer in the gas phase as a showcase system which has the required energetic properties and we measure the time and the efficiency of the energy transfer.

In HeNe, the antenna (He) and receiver (Ne) are weakly bound by the van der Waals force at an equilibrium distance of 3.0 Å. The binding energy is only 2 meV, which is tiny compared to an ionization potential of 21.564 eV of Ne and 24.587 eV of He. The singly excited state He($1s3p$)¹P⁰ at 23.087 eV is the first dipole allowed He state above the Ne ionization threshold, i.e., the first state above the threshold that is quantum-mechanically allowed to couple to the photon field. Thus, HeNe is a good candidate to experimentally search for the predicted antenna effect.

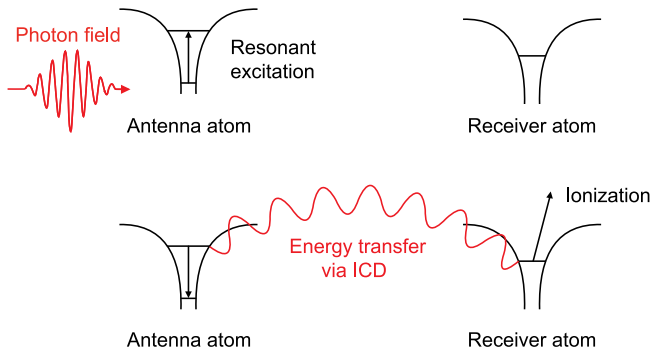


FIG. 1 (color online). Schematic of the antenna mechanism. One atom resonantly absorbs a photon from the field, storing its energy in as an electronic excitation. Before the state decays by fluorescence, the energy is transferred by interatomic Coulombic decay to a neighboring receiver atom with an ionization potential lower than the resonance energy of the antenna atom, where it leads to the emission of an electron. Here, we use He as an antenna atom and Ne as the receiver.

The experiments have been performed at beam line UE112-PGM-1 at the synchrotron radiation facility BESSY (Berlin) in single bunch operation using the COLTRIMS technique [12]. The HeNe dimers were produced by coexpanding an 80%/20% mixture of He and Ne gas through a cooled nozzle at 52 K at a driving pressure of 5 bar. This resulted in a fraction of about 3.2% HeNe dimers and 4.4% Ne₂ dimers. The supersonic gas jet passed two skimmers (0.3 mm diameter) and was crossed with the photon beam at right angles. Ions and electrons created in the interaction region were guided by a weak electric

(7.5 V/cm) and a parallel magnetic (7.8 G) field onto two position sensitive detectors with delay line readout [13]. The time of flight and position of impact of all particles were measured. The time-of-flight spectrum of the measured ions (Fig. 2) shows a clear separation of ^{20,22}Ne⁺ ions, He²⁰Ne⁺ ions, and He²²Ne⁺ ions. In the present experiment, the electron detection and the information on the position of impact of the ions on the ion detector were solely used for background suppression. The photon beam energy was scanned using the monochromator at an energy resolution which was measured *in situ* during the scans to be 1.7 meV (FWHM) by monitoring the strong signal of fluorescence photons from the He(1s3p)¹P⁰ resonance of the 80% of helium atoms in our gas jet (see Fig. 3).

The strength of the antenna effect can most directly be seen in Fig. 2. Off the He resonance, the ratio of Ne⁺ counts to HeNe⁺ counts is about 3.2%, which is the HeNe content in our gas jet. On the resonance [Fig. 2(b)], however, HeNe⁺ is the highest peak. This enhancement of the ionization of HeNe as compared to pure Ne far below the He ionization threshold is caused by the He atom acting as an antenna coupling efficiently to the light field. The counts in the area labeled “dissociation” are Ne⁺ ions with kinetic energies of a few 100 meV which are visible as a halo to the Ne⁺ line. They show the same resonances as the HeNe⁺ signal. We attribute them to dissociation of HeNe⁺ after the electron emission.

For a more detailed investigation of the antenna effect, we show the count rate of HeNe⁺ as function of the photon energy in the vicinity of the He(1s3p)¹P⁰ resonance in

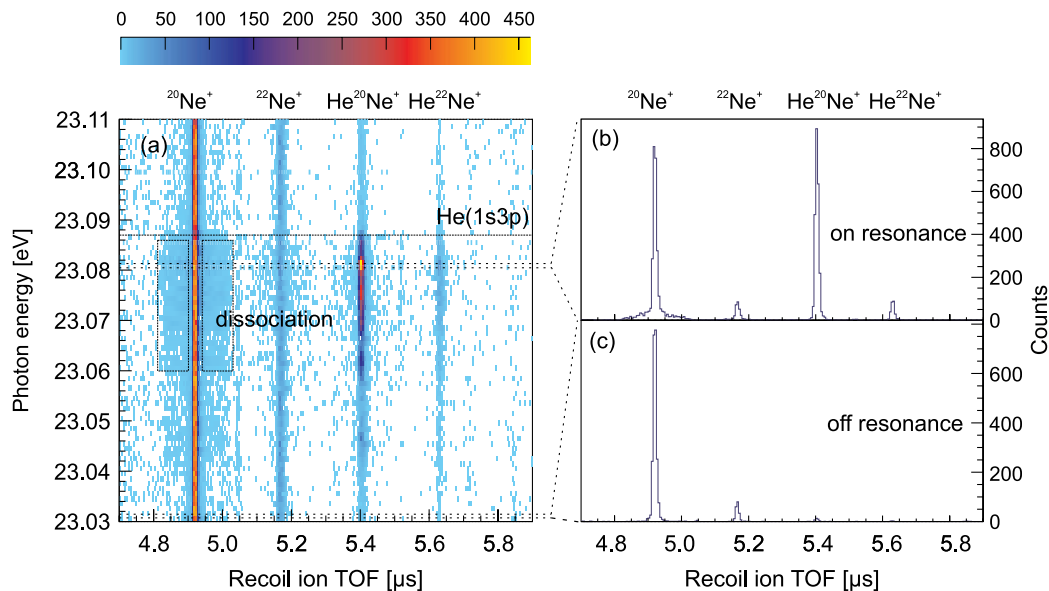


FIG. 2 (color online). Photoionization of a supersonic jet containing He (80%) and Ne (20%) and about 3.2% HeNe dimers. (a) Ion time of flight versus photon energy in the vicinity of the He(1s3p) resonance. (b) Ion time of flight for the photon energy range 23.0805–23.0815 eV (on resonance). (c) Ion time of flight for the photon energy range 23.0305–23.0315 eV (off resonance). (b) and (c) are projections from the data shown in (a).

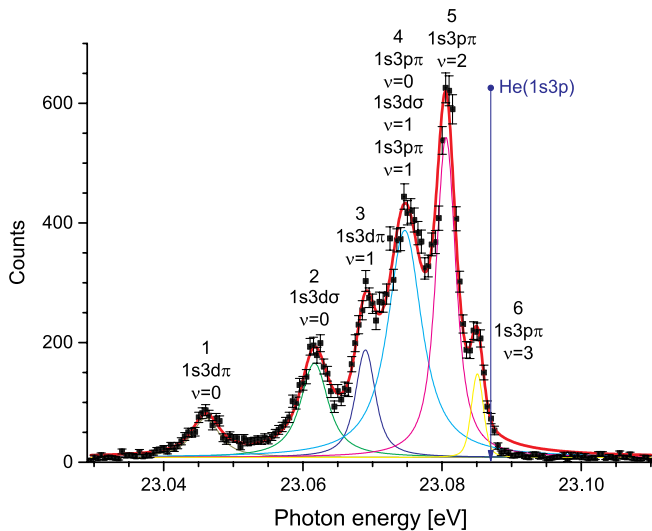


FIG. 3 (color online). HeNe⁺ photoion yield as a function of photon energy in the vicinity of the He(1s3p) resonance. The fits have been made using a multiple Voigt fit (convolution of Lorentzian and Gaussian) with a fixed Gaussian width of 1.7 meV, which is the measured energy resolution of the photon beam. The line indicates the energy of the He(1s3p) in an isolated He atom. For state assignment, see the text and Fig. 4.

Fig. 3. In contrast to the flat energy dependence of the Ne⁺ rate, the HeNe⁺ shows a multiple peak structure slightly below the He(1s3p)¹P⁰ resonance (see also Fig. 5).

This energy shift is induced by the van der Waals environment of the He atom. In addition to the energy shift, the influence of the neighbor also mixes *p* and *d* states, making states of mainly *d* character optically accessible. To identify the peaks, we calculated the potential energy surfaces and

electronic transition moments using the EOM-CCSD(T) method [14] and the EOM-CCSD method [15], respectively, with *v*5z/4s5p5d (He) and *av*5z (Ne) basis sets (Fig. 4). The electronic decay widths were computed using the Fano-Stieltjes method [16] with *v*5z/4s5p5d (He) and *v*5z/4s4p4d (Ne) basis sets employed. The energies and widths of the vibrational states were obtained by diagonalizing the resulting non-Hermitian nuclear Hamiltonian [17]. Table I shows the assignment of all of the experimental peaks based on comparison with this calculation.

The energy absorbed by the He resonance is transferred to the neighboring Ne site from where a 2*p* electron is emitted. The lifetime of the radiative decay of the He(1s3p)¹P⁰ excitation resonance in isolated He is 1.76 ns, corresponding to a width of 2.35×10^{-3} meV [18]. The individual peaks in Fig. 3 are much broader, showing that the resonantly excited state decays much faster in the vicinity of the neon atom than in an isolated helium atom. In order to obtain a lifetime for each of the peaks, we have fitted the spectrum with a sum of six Lorentzians convoluted with a single Gaussian. The width of the Gaussian given by the energy resolution of the photon beam is the same for each of the peaks. An intrinsic check for that width is given online by measuring the fluorescence light from the atomic He(1s3p) component in our jet. Its peak position also provides an *in situ* absolute calibration of our energy scale (see the vertical blue line in Fig. 3).

The temporal behavior of ICD and ICD-like processes is of interest since the first predictions of ICD: The energy transfer time, i.e., the ICD width, depends on the electronic state and on the internuclear distance of the participating atoms or molecules. Furthermore, the number of atomic neighbors that surround the excited particle determines the

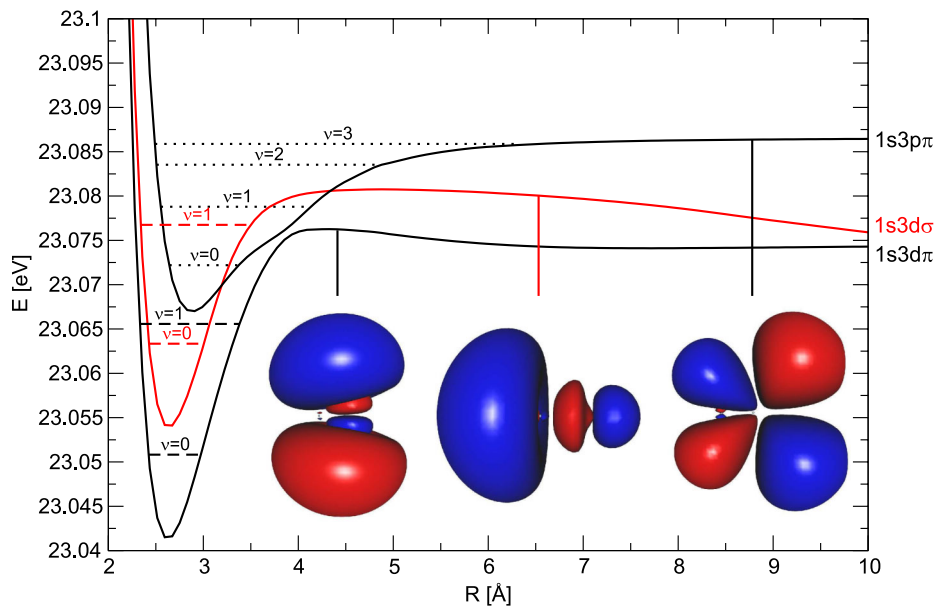


FIG. 4 (color online). Potential energy curves of the excited states of HeNe and the natural orbitals of the excited electron at $R = 3.04 \text{ \AA}$ [15]. The atom on the right is He. The 1s3pσ state is off the scale; it lies about 100 meV above the states shown here.

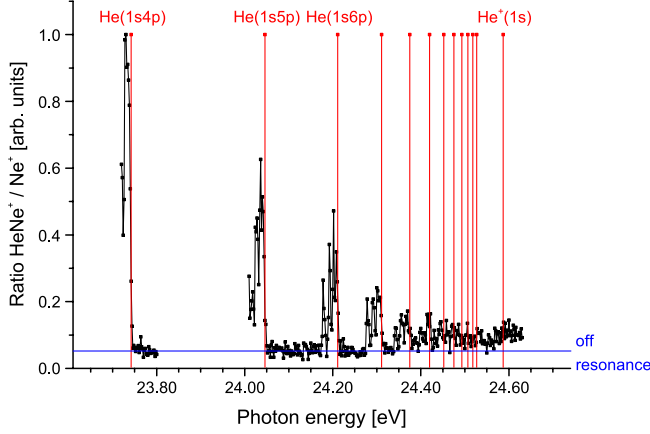


FIG. 5 (color online). HeNe^+ photoion yield as function of photon energy from the $\text{He}(1s4p)$ to the He ionization threshold. The blue baseline results from the nonresonant ionization of the Ne atom.

efficiency of ICD: In some cases, where that number is high, the ICD width becomes comparable to that of a typical Auger decay. In these cases, ICD occurs within a few fs [19]. Pioneering work by Öhrwall *et al.* measured a lifetime of $\text{Ne}^+(2s^{-1})$ in the bulk of larger Ne clusters of 6 fs [20], confirming the time scale on which ICD takes place for the first time. If the excitation mechanism for a decaying state is energetically broadband or the decay width is broader than the vibrational spacing, a coherent vibrational wave packet will be formed upon excitation and the ICD occurs while the excited dimer shrinks or expands, as shown in theoretical work [21–23]. Two recent experiments on ICD of rare gas dimers addressed this scenario. Schnorr *et al.* [24] measured a mean value of the decay time of excited neon dimers integrating over internuclear distances and approximating the nonexponential decay with an exponential decay function in a pump-probe experiment. The first time-resolved measurement of ICD was reported by Trinter *et al.* [25]. They measured the time

dependence of the internuclear distance and were able to show that in the coherent excitation scenario, the decay function of ICD is nonexponential, as predicted [21]. In contrast to the scenario described above, our present experiment in the energy domain uses narrow band excitation and resolves the electronic and the vibrational states. The measured vibrationally resolved widths are shown in Table I. Peaks 4–6 correspond to the second, third, and fourth vibrational levels of $1s3p\pi$ [peak 4 is a mixture of $1s3p\pi$ ($\nu = 0$), $1s3p\sigma$ ($\nu = 1$), and $1s3p\pi$ ($\nu = 1$) states]. It turns out that the lifetime increases from 160 to 1100 fs with increasing vibrational level. This is a direct consequence of the increase of internuclear distance with increasing vibrational level. We find the shortest lifetime for the first vibrational state of $1s3d\pi$. This might be surprising since in an isolated atom, this state would even be dipole forbidden. In the dimer, obviously the Stark mixing between p and d states and the small internuclear distance result in these very short decay times.

Figure 5 displays an extended scan of the photon energy from the $\text{He}(1s4p)$ resonance to the He single ionization threshold. Each of the dipole allowed excited states shows the antenna effect, as the photon energy dependent ratio of HeNe^+ to Ne^+ reveals.

In conclusion, we have experimentally shown that a single atom can act as a highly efficient antenna to absorb energy from a light field and pass the energy to a neighboring receiver atom within a few hundreds of femtoseconds. The vibrationally resolved measurement of the resonance width for a selected electronic state provides a benchmark for future calculations of the underlying energy transfer mechanism of ICD. Our findings yield (to our knowledge) the first vibrationally resolved lifetimes of ICD after narrow band excitation.

We acknowledge the support of RoentDek Handels GmbH. The work was supported by Research Unit 1789 of the Deutsche Forschungsgemeinschaft. The experimentalists thank Alexander Voitkiv and Carsten Müller for

TABLE I. Peak positions, energies, lifetimes, and relative peak intensities for the six peaks in Fig. 3 as well as assigned excited states of HeNe from theory including energies, widths, and relative peak intensities. The experimental numbers have been obtained using a multi-Lorentzian fit convoluted with the Gaussian width of our photon beam, which has been measured independently through the fluorescence light from the atomic $\text{He}(1s3p)$ resonance. The errors of the widths are conservative estimates based on fitting with different seed values and different fitting software.

| Peak | Experiment | | | | Theory | | | |
|------|-------------|---------------------|---------------|-----------|----------------------------|-------------|-------------|-----------|
| | Energy (eV) | Width (meV) | Lifetime (fs) | Intensity | Assignment | Energy (eV) | Width (meV) | Intensity |
| 1 | 23.0460 | 5.0 ± 1.5 | 130 | 5% | $1s3d\pi$ ($\nu = 0$) | 23.050 82 | 3.74 | 7.7% |
| 2 | 23.0617 | 4.5 ± 1.0 | 150 | 13% | $1s3d\sigma$ ($\nu = 0$) | 23.063 34 | 5.68 | 7.2% |
| 3 | 23.0690 | 3.0 ± 1.0 | 220 | 10% | $1s3d\pi$ ($\nu = 1$) | 23.065 57 | 2.90 | 17.4% |
| 4 | 23.0746 | 4.0 ± 1.5 | 160 | 38% | $1s3p\pi$ ($\nu = 0$) | 23.072 20 | 1.41 | 0.9% |
| | | | | | $1s3d\sigma$ ($\nu = 1$) | 23.076 75 | 3.66 | 23.3% |
| | | | | | $1s3p\pi$ ($\nu = 1$) | 23.078 79 | 0.85 | 4.4% |
| 5 | 23.0806 | 2.5 ± 1.2 | 260 | 30% | $1s3p\pi$ ($\nu = 2$) | 23.083 53 | 0.62 | 26.6% |
| 6 | 23.0851 | $0.6^{+1.5}_{-0.3}$ | 1100 | 4% | $1s3p\pi$ ($\nu = 3$) | 23.085 88 | 0.22 | 12.6% |

proposing this experiment and providing a theoretical estimate of the magnitude of the expected effect. We thank Gregor Schiwietz and the team at BESSY for operating the beam line and providing the photon beam.

*doerner@atom.uni-frankfurt.de

- [1] L. Novotny and N. van Hulst, *Nat. Photonics* **5**, 83 (2011).
- [2] U. Fano, *Phys. Rev.* **124**, 1866 (1961).
- [3] B. Najjari, A. B. Voitkiv, and C. Müller, *Phys. Rev. Lett.* **105**, 153002 (2010).
- [4] K. Gokhberg, A. B. Trofimov, T. Sommerfeld, and L. S. Cederbaum, *Europhys. Lett.* **72**, 228 (2005).
- [5] L. S. Cederbaum, J. Zobeley, and F. Tarantelli, *Phys. Rev. Lett.* **79**, 4778 (1997).
- [6] T. Jahnke *et al.*, *Phys. Rev. Lett.* **93**, 163401 (2004).
- [7] S. Marburger, O. Kugeler, U. Hergenhahn, and T. Möller, *Phys. Rev. Lett.* **90**, 203401 (2003).
- [8] U. Hergenhahn, *J. Electron Spectrosc. Relat. Phenom.* **184**, 78 (2011).
- [9] M. Ukai, K. Kameta, K. Shinsaka, Y. Hatano, T. Hirayama, S. Nagaoka, and K. Kimura, *Chem. Phys. Lett.* **167**, 334 (1990).
- [10] W. Kamke, B. Kamke, H. U. Kiefl, and I. V. Hertel, *Chem. Phys. Lett.* **122**, 356 (1985).
- [11] A. Golan and M. Ahmed, *J. Phys. Chem. Lett.* **3**, 458 (2012).
- [12] J. Ullrich, R. Moshhammer, A. Dorn, R. Dörner, L. Ph. H. Schmidt, and H. Schmidt-Böcking, *Rep. Prog. Phys.* **66**, 1463 (2003).
- [13] O. Jagutzki, V. Mergel, K. Ullmann-Pfleger, L. Spielberger, U. Spillmann, R. Dörner, and H. Schmidt-Böcking, *Nucl. Instrum. Methods Phys. Res., Sect. A* **477**, 244 (2002).
- [14] P. Piecuch, S. A. Kurcharski, K. Kowalski, and M. Musial, *Comput. Phys. Commun.* **149**, 71 (2002); P. Piecuch, J. R. Gour, and M. Wloch, *Int. J. Quantum Chem.* **109**, 3268 (2009); K. Kowalski and P. Piecuch, *J. Chem. Phys.* **120**, 1715 (2004).
- [15] The natural orbitals were computed at the EOM-CCSD level using the MOLPRO quantum chemistry program suite; see H.-J. Werner, P. J. Knowles, G. Knizia, F. R. Manby, and M. Schütz, *WIREs Comput. Mol. Sci.* **2**, 242 (2012); MOLPRO, version 2012.1, a package of *ab initio* programs, H.-J. Werner, P. J. Knowles, G. Knizia, F. R. Manby, M. Schütz *et al.*, see <http://www.molpro.net>; T. Korona and H.-J. Werner, *J. Chem. Phys.* **118**, 3006 (2003).
- [16] S. Kopelke, K. Gokhberg, V. Averbukh, F. Tarantelli, and L. S. Cederbaum, *J. Chem. Phys.* **134**, 094107 (2011).
- [17] N. Sisourat, N. V. Kryzhevoi, P. Kolerenc, S. Scheit, and L. S. Cederbaum, *Phys. Rev. A* **82**, 053401 (2010).
- [18] A. Johansson *et al.*, *Eur. Phys. J. D* **22**, 3 (2003).
- [19] V. Averbukh and L. S. Cederbaum, *Phys. Rev. Lett.* **96**, 053401 (2006).
- [20] G. Öhrwall *et al.*, *Phys. Rev. Lett.* **93**, 173401 (2004).
- [21] S. Scheit, L. S. Cederbaum, and H.-D. Meyer, *J. Chem. Phys.* **118**, 2092 (2003).
- [22] N. Sisourat, H. Sann, N. V. Kryzhevoi, P. Kolerenc, T. Havermeier, F. Sturm, T. Jahnke, H.-K. Kim, R. Dörner, and L. S. Cederbaum, *Phys. Rev. Lett.* **105**, 173401 (2010).
- [23] N. Sisourat, N. V. Kryzhevoi, P. Kolerenc, S. Scheit, T. Jahnke, and L. S. Cederbaum, *Nat. Phys.* **6**, 508 (2010).
- [24] K. Schnorr *et al.*, *Phys. Rev. Lett.* **111**, 093402 (2013).
- [25] F. Trinter *et al.*, *Phys. Rev. Lett.* **111**, 093401 (2013).